Chemical Research in Toxicology

Article

pubs.acs.org/crt

DNA Adduct Profiles Predict in Vitro Cell Viability after Treatment with the Experimental Anticancer Prodrug PR104A

Alessia Stornetta,[†] Peter W. Villalta,[‡] Frederike Gossner,[†] William R. Wilson,[§] Silvia Balbo,[‡] and Shana J. Sturla*,[†]

[†]Department of Health Sciences and Technology, ETH Zurich, Schmelzbergstrasse 9, 8092 Zurich, Switzerland

[‡]Masonic Cancer Center, University of Minnesota, 2231 Sixth Street Southeast, Minneapolis, Minnesota 55455, United States

[§]Auckland Cancer Society Research Centre, School of Medical Sciences, The University of Auckland, Auckland 92019, New Zealand

Supporting Information

ABSTRACT: PR104A is an experimental DNA-alkylating hypoxia-activated prodrug that can also be activated in an oxygen-independent manner by the two-electron aldo-keto reductase 1C3. Nitroreduction leads to the formation of cytotoxic hydroxylamine (PR104H) and amine (PR104M) metabolites, which induce DNA mono and cross-linked adducts in cells. PR104A-derived DNA adducts can be utilized as drug-specific biomarkers of efficacy and as a mechanistic tool to elucidate the cellular and molecular effects of PR104A. Toward this goal, a mass spectrometric bioanalysis approach based on a stable isotope-labeled adduct mixture (SILAM) and selected reaction monitoring (SRM) data acquisition for relative quantitation of PR104A-derived DNA adducts in cells was developed. Use of this SILAM-based approach supported simultaneous relative quantitation of 33 PR104A-derived DNA adducts in the same sample, which allowed testing of the hypothesis that the enhanced cytotoxicity, observed by preconditioning cells with the transcription-activating isothiocyanate sulforaphane, is induced by an increased level of DNA adducts induced by PR104H and PR104M, but not PR104A. By applying the new SILAM-SRM approach, we found a 2.4-fold increase in the level of DNA adducts induced by PR104H and PR104M in HT-29 cells preconditioned with sulforaphane and a corresponding 2.6-fold increase in cytotoxicity. These results suggest that DNA adduct levels correlate with drug potency and underly the possibility of monitoring PR104A-derived DNA adducts as biomarkers of efficacy.

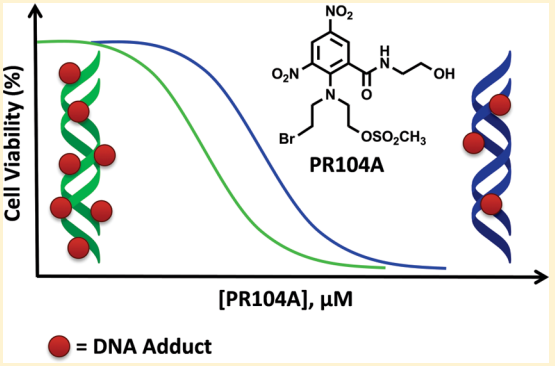

INTRODUCTION

DNA alkylating agents have been used in the clinic for more than 60 years for the treatment of cancer and are still considered first-line medication.[1−3] Their mode of action involves covalent modification to DNA by forming genotoxic DNA adducts that can interfere with replication of cells, especially in rapidly dividing cancer cells. However, a drawback is the typically poor selectivity of these drugs to target cancer cells, which usually results in a wide range of side effects in normal cells of treated patients and arises from processes that are often poorly understood. The use of drug combinations is a common strategy to limit the dose required for each single agent. In addition, reduction of unwanted toxicity can be achieved by developing drugs that are selectively activated by conditions prevalent in cancer, but not in normal tissues such as hypoxia,[4−6] aberrant expression of metabolic enzymes,[7] or oxidative stress.[8]

PR104A is an experimental DNA-alkylating hypoxia-activated prodrug (HAP).[9] This drug is administered as the corresponding phosphate ester PR104, which is systemically hydrolyzed to the alcohol prodrug PR104A. PR104A undergoes metabolic nitroreduction to generate cytotoxic hydroxylamine (PR104H) and amine (PR104M) metabolites (Scheme 1). One-electron reductases such as CYPOR, MTRR, NDOR1, and NOS2A mediate this activation in a process that is inhibited by the presence of oxygen.[10,11] In fact, the initial radical that results from this reduction (**1**, Scheme 1) can be reoxidized by oxygen, whereas under hypoxic conditions, further reduction generates the two major metabolites PR104H and PR104M. These metabolites induce cross-links in DNA.[9,12,13]

It has been found recently that PR104A also can be activated in an oxygen-independent manner by the two-electron aldo-keto reductase 1C3 (AKR1C3, Scheme 1).[14] Evidence for PR104A activation by AKR1C3 includes correlation of protein expression and oxic metabolism of PR104A[14,15] and enhancement of PR104 antitumor activity in AKR1C3-negative tumor xenograft models engineered to overexpress AKR1C3.[14,16] In a recent study, preconditioning of HT-29 colon cancer cells with a low nontoxic dose of sulforaphane (SF), an isothiocyanate

Received: November 2, 2016
Published: January 31, 2017

DOI: 10.1021/acs.chemrestox.6b00412
Chem. Res. Toxicol. 2017, 30, 830−839

Scheme 1. Mechanism of Metabolic Activation of PR104

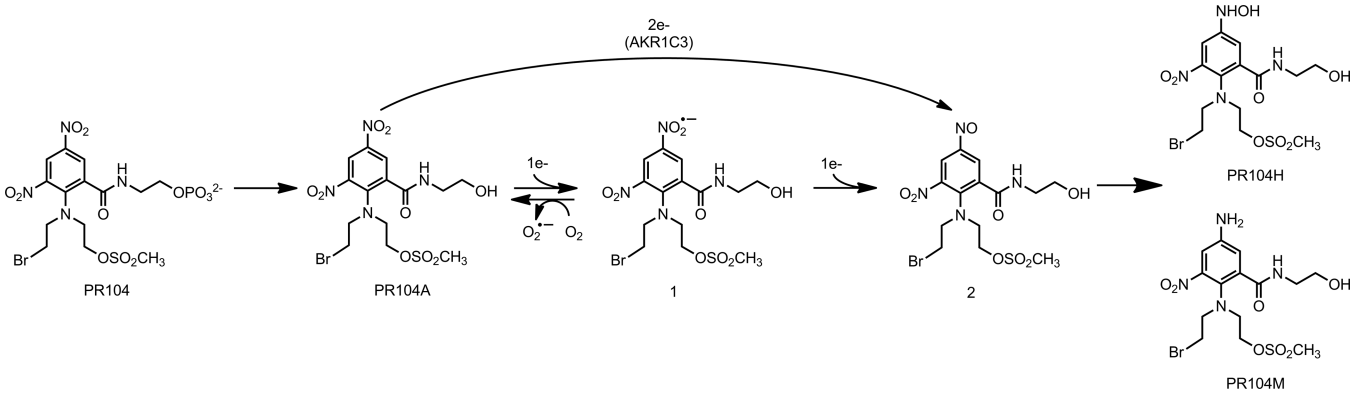

from cruciferous vegetables with the ability to induce xenobiotic-metabolizing and antioxidant enzymes,[17] up-regulated the level of 18 proteins. Among them, AKR1C3 was seven-fold more abundant in SF-treated cells.[18] SF-preconditioning prior to PR104A treatment sensitized HT-29 cells to PR104A and decreased the EC_{50} for cell death by a factor of 3.6 but did not sensitize the immortalized, nontransformed normal human colonic epithelial cells (HCEC).[18] The study focused on the relationship between AKR1C3 levels and cytotoxicity, but the impact of SF on DNA damage induced by PR104A was not investigated.[18]

There is clear evidence that DNA interstrand cross-links contribute to PR104A cytotoxicity, as demonstrated by increased sensitivity of cell lines with genetic defects in cross-link repair[19−21] and correlations between cytotoxicity and cross-link formation as determined by the alkaline comet assay in cell lines in vitro and in xenografts.[12] However, these studies also demonstrated that in cell lines with low rates of metabolic activation of PR104A, cytotoxicity is not accounted for by cross-link formation. Thus, more direct methods for quantitation of DNA damage by PR104A are needed to better understand its mode of toxicity. As an initial step, we recently developed a high-resolution/accurate-mass (HRAM) $LC−MS^3$ DNA adductomic[22] method for screening for PR104A-derived DNA adducts.[13] Both mono and cross-linked DNA adducts induced by the two metabolites, PR104H and PR104M, and by direct alkylation of DNA by PR104A were identified in DNA extracted from cancer cells treated with PR104A.[13] However, to our knowledge, an approach for quantifying PR104A-derived DNA adducts in biological samples does not exist.

Studies involving the application of a strategy for quantifying PR104A adducts are expected to lead to improved understanding of the selectivity factors driving the efficacy of metabolism-activated DNA alkylating agents. Therefore, a goal of this study was to quantify PR104A-derived DNA adducts in cells and evaluate how factors that modulate the responsiveness of cells are reflected in DNA adduct profiles. The strategy was based on the creation of a stable isotope-labeled adduct mixture (SILAM) as a reference standard by enzymatic reduction of PR104A in the presence of DNA. It was used as an internal standard for relative quantitation of adducts by stable isotope dilution mass spectrometry. The SILAM was generated and characterized, and its use as reference standard was validated by measuring adduct levels in purified DNA and in DNA extracted from cells treated with PR104A. LC−MS analysis using the SILAM was carried out via a selected reaction monitoring (SRM) approach targeting 19 DNA adducts induced by PR104A and its metabolites PR104H and PR104M previously detected in cells via DNA adductomic screening. We used the SILAM-SRM approach to test the hypothesis that enhanced cytotoxicity observed by SF-preconditioning of HT-29 cells is induced by increased level of DNA adducts by measuring their levels in colon cancer cells preconditioned with SF.

MATERIALS AND METHODS

Chemicals. PR104A was purchased from Albany Molecular Research, Inc. (Albany, NY). D_4-PR104A was prepared as previously described.[23] R-sulforaphane was purchased from LKT Laboratories (St. Paul, MN). PR104A, d_4-PR104A, and sulforaphane stocks were prepared in DMSO or CH_3OH. Calf thymus DNA (ctDNA) was purchased from Worthington Biochemical Corporation (Lakewood, NJ). AKR1C3 was purchased from United States Biological Life Sciences (Salem, MA). The reference standard [pyridine-d_4]O^6-[4-(3-pyridyl)-4-oxobutyl-1-yl]-2′-deoxyguanosine (d_4-O^6-POB-dG) was prepared as previously described (isotopic purity, 98 at. %D).[24,25] All the other chemicals and enzymes were purchased from Sigma-Aldrich. Cell culture medium and supplements were purchased from Invitrogen (Life Technologies, Switzerland). All solvents used for high performance liquid chromatography (HPLC) and MS analysis were of the purest grade commercially available (≥99.9%).

Cell Culture. HT-29 cells were obtained from the Leibniz-Institute DSMZ GmbH in January 2012 (Braunschweig, Germany). HT-29 cells were grown in DMEM medium with glutaMAX containing 10% fetal bovine serum and 1% penicillin/streptomycin. Immortalized normal diploid human colonic epithelial cells (clone HCEC1CT, abbreviated HCEC) were obtained in August 2011 from Prof. Jerry Shay and grown in a humidified incubator containing 5% CO_2 at 37 °C. The two cell lines have regularly been confirmed to be mycoplasma free by a luminescence detection assay (MycoAlert mycoplasma detection kit, Lonza, Switzerland).

Full details regarding cytotoxicity analysis, reactions of ctDNA with PR104A or d_4-PR104A, validation experiment, and quantitation of dGuo by HPLC for this study can be found in the Supporting Information.

Influence of SF-Preconditioning on DNA Adduct Levels in Cells. Cells were seeded in six-well plates at a density of 5.0×10^5 cells/well and were allowed to attach overnight. Afterward, the medium was replaced with fresh medium containing a final concentration of 2.5 μM SF or 0.1% DMSO (solvent control). After 48 h, the medium was removed, the wells were washed with PBS, and cells were treated with medium containing a final concentration of 150 μM PR104A or 0.1% DMSO (solvent control) and incubated at 37 °C for 4 h. Thereafter, the DNA from intact cells was isolated by extraction with a DNA isolation kit for cells and tissues (Roche, Switzerland). In short, cells were washed with PBS and scraped to one side of the well using a scraper. Lysis buffer (750 μL) was added to each well, cell lysates were collected and sonicated with a Vibra-Cell

DOI: 10.1021/acs.chemrestox.6b00412
Chem. Res. Toxicol. 2017, 30, 830−839

Sonicator (Sonics, CT) using the following conditions: 40% amplitude, 15 cycles at 10 s on and 15 s off. One microliter of proteinase K solution was added to the cell lysates, and samples were incubated for 1 h at 65 °C. Samples were allowed to cool to room temperature, 50 μL of RNase solution was added, and samples were incubated at 37 °C for 1 h. Care should be taken in removing RNA from the sample since adducts from the bases common to DNA and RNA are indistinguishable. A sample of 330 μL of protein precipitation solution was added and samples mixed vigorously, cooled on ice for 5 min, and centrifuged at 16 900*g* for 4 min to form a protein pellet. Supernatants were transferred in clean 2 mL Eppendorf tubes, and 1 mL cold isopropanol was added. Samples were gently mixed until the DNA pellet was visible and centrifuged at 4 °C, 16 900*g* for 10 min. Supernatants were removed without disturbing DNA pellets, which were washed with 1 mL cold EtOH by centrifugation. The resulting DNA pellets were allowed to dry at room temperature for 30 min. DNA was dissolved overnight in 100 μL of nuclease-free water. DNA concentrations of the resulting solutions were determined with a NanoDrop 1000 spectrometer (Thermo Scientific, Waltham, MA). The 10 mM Tris-HCl/5 mM $MgCl_2$ buffer (pH 7) was added to a final volume of 900 μL. Samples were spiked with the SILAM (1.5 μL) and thermally hydrolyzed at 80 °C for 1 h. The sample containing the highest amount of DNA was used as reference to calculate the units (U, corresponding to the amount of the enzyme that catalyzes the conversion of 1 μmol of substrate per min) of enzymes for enzyme hydrolysis. Then 600 U/mg DNA of DNase I was added, and samples were incubated overnight at 37 °C. Afterward, additional DNase I (600 U/mg DNA) was added together with phosphodiesterase I (20 mU/mg DNA) and alkaline phosphatase (240 U/mg DNA), followed by incubation at 37 °C overnight. The enzymes were removed by centrifugation using a Centrifree ultrafiltration device (MW cutoff 30 000 atomic mass unit (amu); Merck Millipore, Cork, Ireland). An aliquot (60 μL) was taken from each sample for the analysis of deoxyguanosine (dGuo) by HPLC. A solution of the same buffer and enzymes was used as a negative control. Hydrolysates were purified by solid-phase extraction (SPE) on a Strata-X cartridge (30 μm, Phenomenex, Torrance, CA). Cartridges were preconditioned with 3 mL of CH_3OH and 1 mL of H_2O. The samples were loaded on the cartridge, washed with 1 mL of 40% CH_3OH, and eluted with 600 μL of 80% CH_3OH in H_2O. The eluted fractions were evaporated to dryness and stored at −20 °C. Prior to LC−MS analysis, samples were dissolved in 20% CH_3OH in H_2O to a final volume of 10 μL. All steps of the protocol were performed using silanized glass tubes.

Chromatography (for LC−MS). Corresponding to DNA amounts ranging from 1−8 μg (cell samples) or 15−50 μg (ctDNA samples), 0.5, 2, or 5 μL of hydrolyzed, SPE-purified, and reconstituted sample was injected onto a nanoACQUITY UPLC (Waters Co., Milford, MA) system equipped with a 5 μL injection loop. Separation was performed with a capillary column (75 μm ID, 10 cm length, 15 μm orifice) created by hand packing a commercially available fused-silica emitter (New Objective, Woburn MA) with 5 μm Luna C18 bonded separation media (Phenomenex, Torrance, CA). The flow rate was 1000 nL/min for 5.5 min, then decreased to 300 nL/min with a 50 min linear gradient from 2−50% CH_3CN in 5 mM NH_4OAc aqueous buffer (pH 5.5), an increase to 98% CH_3CN in 3 min, with a 2 min hold and a 5 min re-equilibration at 1000 nL/min at 2% CH_3CN. The injection valve was switched at 5.5 min to remove the sample loop from the flow path during the gradient.

Mass Spectrometry. Data-dependent CNL-MS^n scanning with nanoelectrospray was carried out using an LTQ Orbitrap Velos instrument (Thermo Scientific, Waltham, MA). The nanoelectrospray source voltage was 2.0 kV, and the capillary temperature was 350 °C. The ion focusing and transfer elements of the instrument were adjusted for maximum signal intensity by using the automated instrument tuning feature while the background ion signal of *m/z* 371.1 (decamethylcyclopentasiloxane) was monitored to create the tune file used for data analysis. The S-Lens RF level setting was 49%. Data-dependent MS^3 analysis was performed with repeated full scan detection followed by MS^2 acquisition and constant neutral loss triggering of MS^3 fragmentation. Full scan (200−2000 Da) detection was performed using the Orbitrap detector at a resolution of 60 000 (at *m/z* 400) with one microscan (one mass analysis followed by ion detection), automatic gain control (AGC) target settings of 1×10^6, and a maximum ion injection time setting of 100 ms. MS^2 fragmentation was performed in the ion trap on the three most intense full scan ions listed in a parent mass list with Orbitrap detection at a resolution of 7500, AGC of 2×10^5, one microscan, maximum ion injection time of 100 ms, and full scan injection waveforms enabled. The parent mass list was composed of 298 masses corresponding to $[M + H]^+$ ions of anticipated mono and cross-linked DNA adducts from reaction of the four DNA bases with PR104A, PR104H, PR104M, or the corresponding d4-analogues. MS^2 fragmentation parameters were as follows: 3 amu isolation width, normalized collision energy of 35, activation *Q* of 0.25, and activation time of 10 ms. Data-dependent parameters were as follows: triggering threshold of 10 000, repeat count of one, exclusion list size of 500, exclusion duration of 60 s, and exclusion mass width of ±5 ppm. MS^3 HCD fragmentation (2 amu isolation width, normalized collision energy of 35, activation time of 0.1 ms) with Orbitrap detection at a resolution of 7500 was triggered upon observation of neutral losses (±5 ppm) of 116.0474, 151.0494, 135.0545, 126.0429, and 111.0433 amu between the parent ion and one of the 50 most intense product ions from the MS^2 spectrum, provided a minimum signal of 1000 was observed. The following MS^3 parameters were used: one microscan, AGC target setting 2×10^5, maximum ion injection time of 100 ms. All spectra were acquired using the background ion signal of *m/z* 371.10124 amu (decamethylcyclopentasiloxane) as a lock mass. Instrument sensitivity was checked before each analysis by injection of 10 fmol of labeled standard (d_4-O^6-POB-dG) and by integration of the observed peak in the extracted ion chromatogram of the exact mass of its parent ion.

For SRM scanning, samples were analyzed by nanoelectrospray in SRM mode on a TSQ Vantage instrument (Thermo Scientific, Waltham, MA). The nanoelectrospray source voltage was 1.6 kV, and the capillary temperature was 300 °C. Q2 CID gas pressure, 1.0 mTorr; collision gas, argon; scan width, *m/z* 0.100; scan time, 0.050 s; collision energy, 20 V (base adducts) or 15 V (nucleoside adducts); Q1 peak width, 0.70 amu; and Q3 peak width, 0.70 amu. Mass transitions monitored were *m/z* 446.2−311.1, *m/z* 462.2−311.1, *m/z* 476.2−341.1, *m/z* 492.2−341.1, *m/z* 494.1−359.1, *m/z* 510.1−359.1, *m/z* 554.1−403.0, *m/z* 562.2−446.2, *m/z* 563.2−428.1, *m/z* 579.2−428.1, and 579.2−444.1, *m/z* 592.2−476.1, *m/z* 595.2−444.1, *m/z* 608.2−492.2, *m/z* 611.3−460.1, *m/z* 625.2−474.2, *m/z* 695.3−579.2, *m/z* 711.3−595.2, and *m/z* 741.3−625.2, and the 19 isotope labeled corresponding standards (+ 4 amu). The tune file used for the analysis was created by maximizing signal at conditions similar to those present during DNA adduct elution (300 nL/min, 50% CH_3CN, mass range 400−800 amu). Instrument sensitivity was checked before each analysis by injection of the same sample containing seven PR104A-induced DNA adducts and by comparison of the peak areas.

Statistical Analysis. A *t* test was used to verify whether SF-preconditioned and control samples were statistically significantly different from each other (GraphPad Prism 6).

RESULTS

Creation and Characterization of the Stable Isotope-Labeled Adduct Mixture (SILAM). The SILAM to be used for relative quantitation was generated by reacting purified DNA from calf thymus (ctDNA) with d_4-labeled PR104A in the presence of AKR1C3 and NADPH. Following a 24 h reaction, the DNA was precipitated, the residual d_4-PR104A removed by chloroform/isoamyl alcohol extraction, the DNA hydrolyzed, and the hydrolysate enriched by solid phase extraction. The resulting mixture then was characterized by a previously reported HRAM LC−MS^n DNA adductomic approach.[13] Briefly, repeated full scan detection followed by MS^2 acquisition and constant neutral loss triggering of MS^3 fragmentation (data-dependent scanning) to confirm the presence of a DNA

DOI: 10.1021/acs.chemrestox.6b00412
Chem. Res. Toxicol. 2017, 30, 830−839

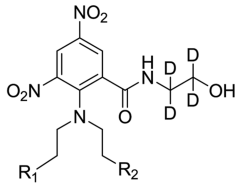

d_4-PR104A-adducts

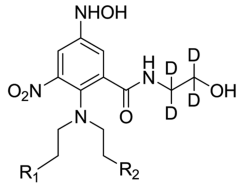

d_4-PR104H-adducts

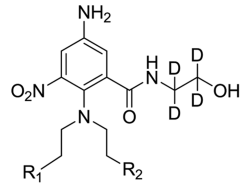

d_4-PR104M-adducts

Analyte	Proposed alkylating species	Neutral loss that triggered an MS^3 event	Mass $[M+H]^+$	Retention time[a] (min)	Peak area[b]	Relative peak area (fold increase)	R_1	R_2
1	PR104M	A	450.2146	11.70	7.32E+08	4067	OH	A
2	PR104H	A	466.2095	12.70	7.19E+07	399	OH	A
3	PR104A	C	474.1437	25.66	1.79E+06	10	Cl	C
4	PR104A	A	480.1888	16.59	2.40E+08	1333	OH	A
5	PR104H	G	482.2044	13.97	1.34E+07	74	OH	G
6	PR104M	G	484.1756	18.32	1.03E+06	6	Cl	G
7	PR104A	G	496.1837	17.50	6.18E+08	3433	OH	G
8	PR104A	A	498.1549	21.34	3.77E+07	209	Cl	A
9	PR104A	G	514.1498	21.51	2.62E+08	1456	Cl	G
10	PR104A	C	518.0931	26.47	1.82E+06	10	Br	C
11	PR104M	dR	542.2507	11.68	1.62E+07	90	OH	dC
12	PR104A	G	558.0993	22.23	4.35E+08	2417	Br	G
13	PR104M	dR	566.2619	8.43	2.98E+07	166	OH	dA
14	PR104M	A	567.2585	8.70	1.76E+07	98	A	A
15	PR104A	dR	572.2249	16.12	5.69E+06	32	OH	dC
16	PR104M	G	583.2534	11.68	3.46E+06	19	A	G
17	PR104H or PR104M	A	583.2534	12.61	2.67E+06	15	A	G or A
18	PR104A	dR	587.2246	21.10	1.34E+06	7	OH	dT
19	PR104A	dR	590.1910	20.27	1.74E+06	10	Cl	dC
20	PR104A	dR	596.2361	15.00	1.55E+07	86	OH	dA
21	PR104H or PR104M	G	599.2484	13.84	4.06E+07	226	G	G or A
22	PR104A	dR	605.1907	24.58	2.30E+05	1	Cl	dT
23	PR104A	dR	612.2310	19.83	9.73E+06	54	OH	dG
24	PR104A	dR	614.2022	18.88	1.55E+06	9	Cl	dA
25	PR104H	G	615.2433	13.84	6.04E+05	3	G	G
26	PR104A	G	629.2225	15.58	1.40E+08	778	G	G
27	PR104A	dR	630.1971	23.85	3.59E+06	20	Cl	dG
28	PR104A	dR	634.1405	20.78	1.21E+07	67	Br	dC
29	PR104A	dR	635.1245	24.27	1.80E+05	1	Br	deam-dC
30	PR104A	dR	658.1517	20.04	9.10E+06	51	Br	dA
31	PR104A	dR	674.1466	24.60	2.33E+06	13	Br	dG
32	PR104H	dR	699.3008	12.25	2.41E+07	134	dA	A
33	PR104M	dR	715.2957	16.29	2.07E+07	115	dG	G

[a]Retention time at which the MS^3 fragmentation event was triggered; [b]Peak area resulting from injection of 1 μL of the reconstituted 80% CH_3OH fraction, corresponding to 15 μg of the initial DNA amount used. Abbreviations: dR, 2'-deoxyribose; G, guanine; A, adenine; C, cytosine; T, thymine; dG, deoxyguanosine; dA, deoxyadenosine; dC, deoxycytidine; dT, thymidine; and deam-dC, deaminated dC.

Figure 1. D_4-labeled PR104A DNA adducts detected by MS^3 fragmentation present in the stable isotope-labeled adduct mixture (SILAM).

adduct was performed by nanoelectrospray on an LTQ Orbitrap Velos. Data-dependent MS^2 fragmentation was performed on the three most intense full scan ions listed in a parent mass list composed of d_4-labeled masses of the $[M + H]^+$ ions of anticipated mono and cross-linked DNA adducts induced in the four DNA bases by PR104A, PR104H, and PR104M. MS^3 fragmentation was performed upon observation of the accurate mass neutral loss of the four DNA bases (G, 151.0494 amu; A, 135.0545 amu; T, 126.0429 amu; and C, 111.0433 amu) or of the 2′-deoxyribose (116.0474 amu).[13]

A total of 33 isotope-labeled mono and cross-linked DNA adducts induced by PR104A, PR104H, and PR104M were detected in the SILAM by the presence of an MS^3 fragmentation event (Figure 1, base peak accurate mass extracted ion chromatograms for the 33 detected adducts are shown in Figure S1 in the Supporting Information). Their

DOI: 10.1021/acs.chemrestox.6b00412
Chem. Res. Toxicol. 2017, 30, 830−839

abundances in the SILAM, estimated by integration of the peak areas, varied by three orders of magnitude between the most to the least abundant adducts (Figure 1). For example, the deaminated nucleoside monoadduct that resulted from cytosine alkylation by PR104A (m/z 635.1245, analyte 29 in Figure 1) was among the less abundant adducts, whereas the hydrolyzed monoadduct that resulted from N7-guanine alkylation by PR104A (m/z 496.1837, analyte 7 in Figure 1) was among the most abundant adducts present.

Analytical Validation of SILAM. The SILAM-based method for relative quantitation of PR104A-derived DNA adducts was validated by comparing calculated and measured DNA adduct concentrations in samples obtained by diluting a single ctDNA sample that had been reacted with PR104A into four samples containing increasing amounts of DNA. All samples were spiked with the same amount of the SILAM, processed as described in the Materials and Methods section, and analyzed by LC−MS. Results of this quantitation validation experiment involving purified DNA are shown in Figure 2 for a representative DNA cross-link adduct (m/z 625) in samples analyzed with two different DNA adductomic approaches: the HRAM LC−MS^3 approach and a new developed SRM approach targeting 19 DNA adducts induced by PR104A, PR104H, or PR104M. For the PR104A-induced cross-linked DNA adduct, the slope and R^2 estimates were extrapolated and a very good correlation between calculated DNA concentration and measured adduct concentration was found for both LC−MS approaches used (Figure 2). In addition to the cross-link adduct of m/z 625, 8 versus 12 additional adducts were present in the ctDNA samples and quantified by the HRAM and SRM approaches, respectively (structures, correlation plots, slopes, and R^2 values for these adducts can be found in Figures S2−S4 in the Supporting Information). These adducts comprised mono and cross-linked adducts induced by the two metabolites or by direct alkylation by PR104A. For all these adducts and for both the analytical approaches (HRAM vs SRM), as expected, a very good correlation was found between calculated DNA and measured adduct concentrations (slope and R^2 estimates ranged from 0.92−1.12 and 0.97−1.00 for the HRAM validation, and from 0.98−1.16 and 0.89−1.00 for the SRM targeted validation, Figures S2−S4).

Because of the higher number of adducts detected and the ease of use and sensitivity of quantitation of triple quadrupole instrumentation operating in SRM mode, we decided to use this system with the SILAM for relative quantitation. Thus, the accuracy of quantitation of this approach was evaluated for DNA extracted from PR104A-treated cells. In an analogous experiment to that performed with purified DNA, HT-29 cells were treated with PR104A (500 μM final concentration), and the DNA was extracted and divided into two samples with one containing 50% more DNA than the other. These samples were spiked with the same amount of the SILAM, the DNA adducts enriched by solid phase extraction, and samples were analyzed by nanoLC−ESI−MS/MS in SRM mode. A total of eight DNA adducts induced by PR104A and PR104M were quantified. Deviations of the measured DNA adduct concentrations from the calculated DNA amounts were between 0.6 and 5.5% (Table S1).

Profiles of PR104A-Derived DNA Adducts in Cells Preconditioned with Sulforaphane (SF). The newly developed SILAM approach was used to compare levels of PR104A-derived DNA adducts in colon cancer cells preconditioned with SF. First, the experiments demonstrating increased

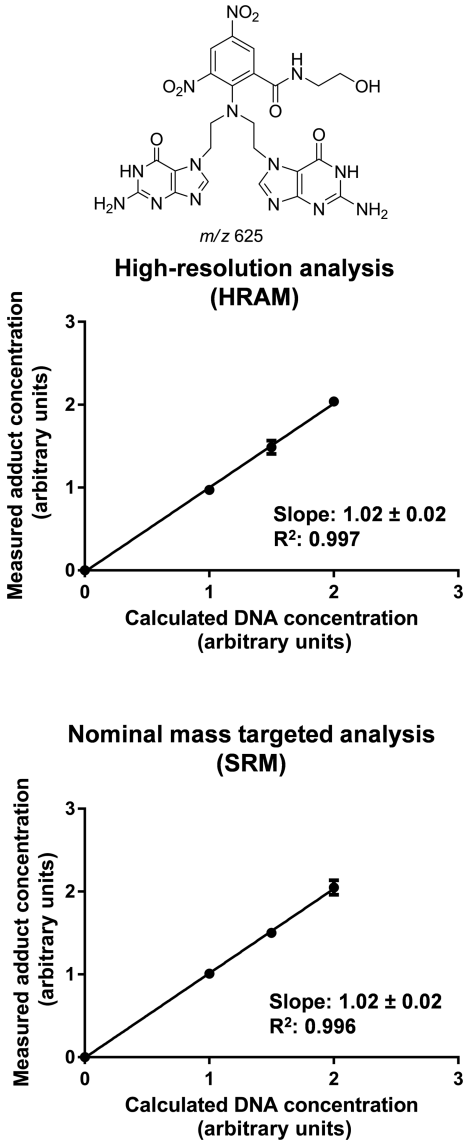

Figure 2. Validation of the SILAM for relative quantitation of the PR104A-derived DNA adducts (shown here for the DNA cross-link with m/z 625 as a representative example) in purified DNA treated with PR104A (100 μM final concentration) for 24 h. Analysis was performed with both a high-resolution analysis (HRAM) and with a nominal mass targeted analysis (SRM). Error bars represent the standard deviation derived from three replicate experiments. Lines represent linear regressions.

sensitivity of HT-29 cells for PR104A treatment upon SF-preconditioning and the lack of alteration in sensitivity of HCEC cells, which was observed previously, were repeated, and the results confirmed (Figure S5).[18] There was an increase in sensitivity of HT-29 cells toward PR104A (EC_{50} value 20.5 μM vs 7.9 μM for the nontreated vs SF-treated cells), which represented a 2.6-fold decrease, while there was no change in the case of HCEC cells (Figure S5). However, the relationship between adduct formation and the positive interaction of SF and PR104A was unknown.

PR104A-derived DNA adducts were therefore quantified in HT-29 and HCEC cells preconditioned with a SF concentration corresponding to the EC_{10} value derived for SF in HT-29 cells when individually tested. The analysis was performed by spiking the samples containing DNA extracted from HT-29

DOI: 10.1021/acs.chemrestox.6b00412
Chem. Res. Toxicol. 2017, 30, 830−839

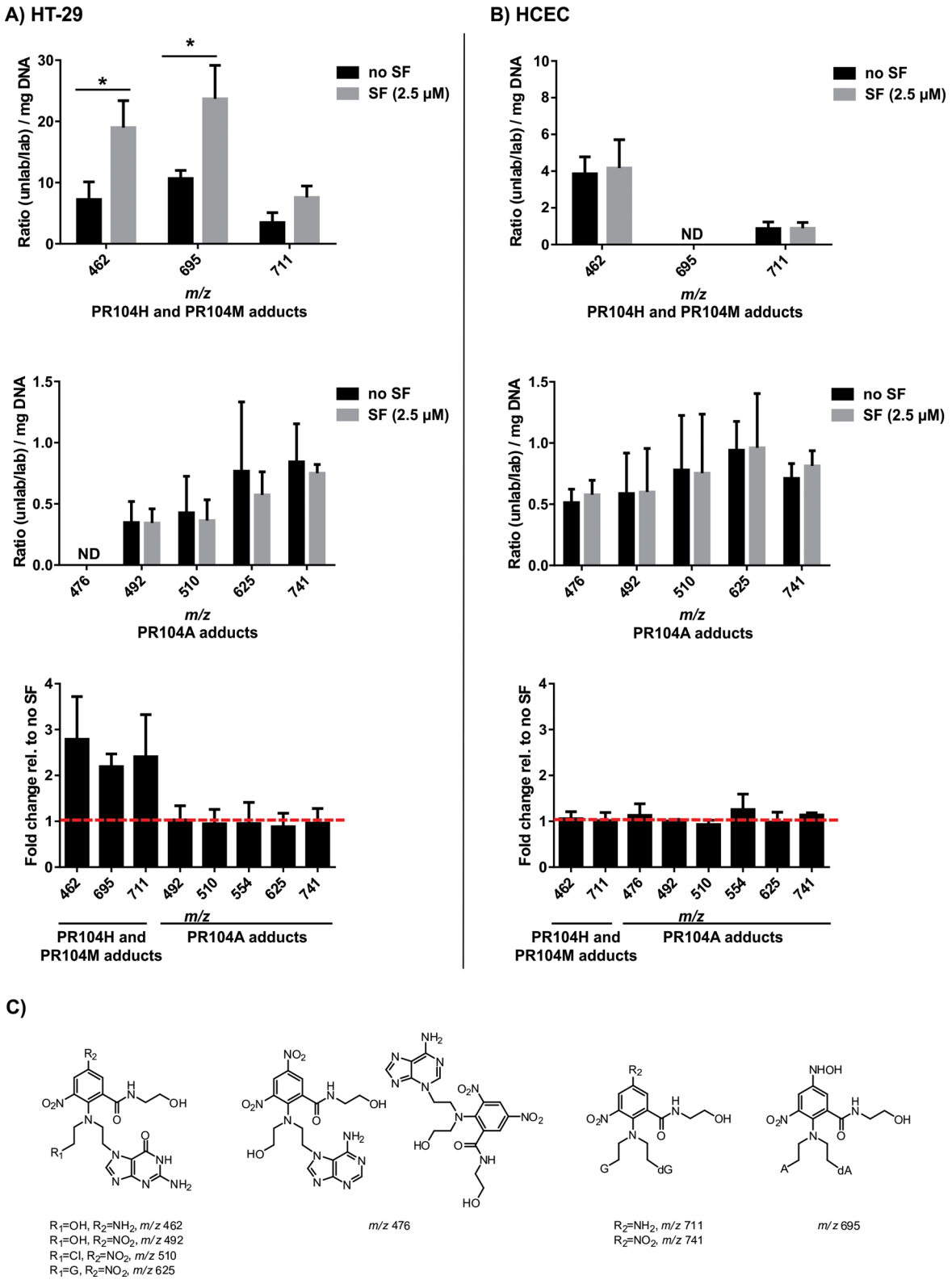

Figure 3. PR104A-derived DNA adduct levels and fold change relative to SF-untreated controls in (A) HT-29 and (B) HCEC cells upon SF-preconditioning versus controls. Asterisks above the bars represent statistical significance (*t* test, $p < 0.05$), whereas ND represents nondetects. (C) Proposed structures of PR104A-derived DNA adducts quantified in HT-29 and HCEC cells.

or HCEC cells preconditioned with SF and treated with PR104A with the SILAM prior to hydrolysis and DNA adduct enrichment by solid phase extraction. The analysis was performed in SRM mode targeting 19 PR104A-, PR104H-, and PR104M-induced DNA adduct masses. The relative amount of each DNA adduct was calculated by dividing the ratio of the peak areas corresponding to the unlabeled and labeled adducts by the total DNA concentration of each sample. The total DNA was determined by quantitation of 2′-deoxyguanosine (dGuo) by HPLC. Negative control samples

DOI: 10.1021/acs.chemrestox.6b00412
Chem. Res. Toxicol. 2017, 30, 830−839

were samples containing buffer and enzymes used for the DNA hydrolysis and a sample containing DNA extracted from cells treated with SF only. None of the 19 targeted adducts was observed in these samples.

A total of seven mono and cross-linked DNA adducts resulting from PR104A, PR104H, or PR104M were observed and quantified in both cell lines (Figure 3). Some adducts were detected in both cell lines (m/z 462, 711, 492, 510, 625, and 741), whereas two adducts could be detected in one cell line only (m/z 695 in HT-29, and m/z 476 in HCEC, Figure 3). DNA adducts detected included both mono and cross-linked adducts from PR104A (m/z 476, 492, 510, 625, and 741) and its reactive PR104H and PR104M metabolites (m/z 462, 695, and 711, Figure 3C). SF-preconditioning of HT-29 cells increased the amount of DNA adducts induced by the two metabolites PR104H and PR104M, but not of the DNA adducts resulting from direct alkylation by PR104A (Figure 3A). This increase was statistically significant for two of the metabolite-induced DNA adducts quantified in HT-29 cells (Figure 3A). On the other hand, no alteration of metabolite-induced DNA adduct levels upon SF-preconditioning was observed in HCEC cells (Figure 3B). These data support a direct role of DNA adducts in PR104A toxicity and, moreover, support a mechanistic model for the basis of how SF-preconditioning sensitizes HT-29 cells.

DISCUSSION

A potential strategy to further our understanding of the mechanism of action of the prodrug PR104 and to support biomarker-based personalized strategies for its clinical use involves using DNA adducts as drug-specific biomarkers of efficacy. DNA adducts have been used as mechanism-based biomarkers of exposure to carcinogens for hazard identification and risk assessment and for the estimation of human exposure to occupational, environmental, and dietary chemicals.[26] Examples of anticancer drug classes for which the relationship between DNA adducts and response were studied in vitro and in vivo include platinum-based drugs, nitrogen mustards, and minor groove binding agents.[27] The advantage of monitoring drug−DNA adducts as biomarkers of efficacy relies on their drug-specificity and stability in DNA. The challenge relies on the ability to identifying and quantifying them in biological samples since DNA adducts are usually present in animal and human tissues in extremely low abundance compared to unmodified nucleobases (on the order of 0.01−10 adducts per 10^8 unmodified nucleobases if induced by carcinogens,[20,21] and on the order of 1−1000 adducts per 10^8 unmodified nucleobases if induced by anticancer drugs). In this study, a DNA adductomic approach for the quantitation of previously detected PR104A-derived DNA adducts[13] in cells was developed and validated for allowing relative quantitation of PR104A-DNA adducts in purified DNA and in DNA extracted from cells treated with PR104A. With the developed approach, DNA adduct levels were measured in cells preconditioned with the bioactive food compound sulforaphane (SF), and the relationship between PR104A-derived DNA adducts and cell viability response in vitro was investigated. We found a ∼2.4-fold increase in the level of DNA adducts induced by the two metabolites PR104H and PR104M in SF-preconditioned HT-29 cells. This increase was in good agreement with the 2.6-fold increase in cytotoxicity in HT-29.

To circumvent limitations to rapid development and validation of DNA adduct monitoring strategies for clinical applications, we used an unconventional strategy for adduct quantitation that does not require synthesis of labeled standard for each adduct, but rather involves the creation of a stable isotope-labeled adduct mixture (SILAM). Quantitation of DNA adducts usually involves spiking the samples at an early stage of the sample preparation with a chemically synthesized stable isotope-labeled internal standard of a DNA adduct of interest.[28] The isotope-labeled internal standard accounts for losses occurring during sample preparation, ion suppression from the sample matrix, and instrument variability during LC−MS analysis.[28,29] Addition of a known concentration of the stable isotope labeled standard allows one to calculate the accurate concentration of the adduct of interest in the sample, which results in absolute quantitation.[28] Absolute quantitation approaches depend on the availability of stable isotope labeled internal standards for adducts of interest, the synthesis of which can be time-consuming and challenging depending, for example, on adduct structure and stability and on the cost of the stable isotope-labeled starting material. The results described herein demonstrate that using a SILAM reference standard can allow for the simultaneous relative quantitation of several PR104A-derived DNA adducts in the same sample and account for adduct losses during sample preparation and ion suppression from sample matrix during LC−MS analysis.

On the basis of triggered MS^3 fragmentation events for neutral loss of a DNA adduct feature, and absence of this fragmentation event in the control samples, the SILAM contained 33 detectable isotopically labeled mono and cross-linked DNA adducts induced by PR104A including adducts ascribed to alkylation by the metabolites PR104H and PR104M (Figure 1). The assignment of adducts as PR104A versus PR104H or PR104M adducts was on the basis of their accurate masses and fragmentation patterns. The composition of the SILAM suggests the potential for deriving relative amounts of up to 33 PR104A-derived DNA adducts simultaneously depending on whether they are present in biological samples. The use of SILAM for relative quantitation of PR104A-derived DNA adducts was demonstrated by the strong correlation between calculated and measured DNA adduct concentrations in a validation experiment involving PR104A-treated purified DNA and DNA extracted from PR104A-treated cells (Figures 2 and S2−S4, and Table S1).

The HRAM Orbitrap analysis used for the initial PR104A-adduct discovery work[13] also provided good relative quantitation in purified DNA samples spiked with SILAM, in which nine adducts from the list of target adducts were quantified. This result is comparable to the 13 adducts measured by triple quadrupole SRM-targeted analysis and is encouraging for future combined adduct discovery/relative quantitation investigations of this type. However, the SILAM triple quadrupole SRM-targeted approach provided for relative quantitation of more of the targeted adducts and is a simpler, more widely available technology and therefore was chosen for the evaluation of PR104A-derived adducts in treated cells. Its accuracy and precision was evaluated for DNA extracted from PR104A-treated cells, and the results further supported the suitability of the SILAM for relative quantitation of PR104A-derived DNA adducts (Table S1).

The SILAM-SRM approach has the potential to be used for monitoring DNA adducts induced by DNA alkylating drugs in patient samples. For this purpose, biological samples such as tumor biopsy, circulating cancer cells, and surrogate tissues could be collected from patients undergoing chemotherapy and

DOI: 10.1021/acs.chemrestox.6b00412
Chem. Res. Toxicol. 2017, 30, 830−839

DNA adducts analyzed by SILAM-SRM. Alternatively, the DNA adducts can be quantified by the SILAM-SRM approach in peripheral blood mononuclear cells or tumor biopsy isolated from patients treated with a microdose of the DNA alkylating drug, whereas another potential scenario for sensitivity testing might involve ex vivo exposure of cancerous or normal surrogate cells to the DNA alkylating drug with evaluation of adduct formation.[27]

We further evaluated the method in the context of characterizing DNA adduct profiles in colon cancer cells preconditioned with SF prior to PR104A treatment. We previously reported that the increase in PR104A activity in HT-29 cells upon preconditioning with SF results from an increase in abundance and activity of the enzyme AKR1C3.[18] Increase in gene expression of AKR1C3, as for the other xenobiotic-metabolizing and antioxidant enzymes modulated by SF,[30−32] is mediated by the transcription factor nuclear factor erythroid 2-related factor 2 (Nrf2).[33] Thus, SF reacts with cysteine residues of the Nrf2 repressor Keap1, which results in nuclear translocation of Nrf2 and binding of the transcription factor to DNA.[33] Higher amount of AKR1C3 is thought to increase the level of drug activation and the production of reactive hydroxylamine (PR104H) and amine (PR104M) metabolites, as demonstrated previously by analysis of the metabolites by LC−MS/MS in HCT116 cells engineered to express AKR1C3.[14] The expectation was that SF-induced AKR1C3 would lead to increased metabolite-induced DNA adducts; on the other hand, DNA adducts resulting from direct alkylation by PR104A should not depend on the level of AKR1C3. Therefore, we expected the levels of direct adducts to be invariant between SF-preconditioned and directly treated cells.

This model was indeed supported by the results of this study, in which preconditioning HT-29 cells with SF led to an increase in the levels of DNA adducts induced by the two metabolites PR104H and PR104M but did not affect the level of DNA adducts resulting from direct alkylation by PR104A (Figure 3A). The average increase in metabolite-induced DNA adducts relative to SF-untreated control in HT-29 cells (∼2.4 fold) matched closely the 2.6-fold decrease observed in the EC_{50} value derived from the cell viability dose−response curve in HT-29 cells (Figure S5). Among the three SF-modulated metabolite-induced DNA adducts quantified in HT-29 cells, the one with m/z 462 was attributed to a hydrolyzed monoadduct induced by the reaction of PR104M with a guanine, whereas the other two adducts with m/z 695 and 711 were attributed to cross-linked adducts induced by PR104H with two adenines, and by PR104M with two guanines, respectively (Figure 3C). An evaluation of the individual contribution of these adducts to cytotoxicity and therefore a conclusion regarding which of these adducts are more biologically relevant for the observed cytotoxicity is challenging, due to the heterogeneity of DNA alkylation, that is, it is not possible to induce and observe the cytotoxic effects of one adduct at a time, rather all are formed in concert. Despite the ability of interstrand cross-links to prevent DNA strand separation and block DNA replication and transcription,[34] their formation is much lower than that of monoadducts. Therefore, the overall cytotoxicity may result from a combination of effects from mono and cross-linked adducts, and further research outside the scope of the current study, such as using cells with the selective capacity to remove particular adducts, would be of interest to resolve this open question.

Finally, it was anticipated that there would be no change in adduct levels when HCEC cells were preconditioned with SF given the slight AKR1C3 induction and no significant increase in AKR1C3 activity in these nontumorigenic colonic mucosal cells.[18] Again, this assertion could be confirmed (Figure 3B). To investigate reasons for different cytotoxicity responses in HT-29 versus HCEC cells, Erzinger et al. measured the cellular uptake of SF but found no significant differences in SF uptake between the two cell lines. Therefore, one may speculate that differences in induction of AKR1C3 in HT-29 and HCEC cells result from differences in the level of Nrf2, or in the ability to translocate Nrf2 into the nucleus to reach DNA. Nevertheless, the absence of change in adduct levels in HCEC cells upon SF-preconditioning measured in this study further supports the causative relationship between induction of PR104A-derived adducts and cytotoxicity.

CONCLUSIONS

In conclusion, we established in this study evidence for a direct relationship between SF-preconditioning of cells, the abundance of DNA adducts derived from the experimental nitrogen mustard prodrug PR104A, and PR104A cytotoxicity in a cancer and in a noncancerous cell line. This insight was enabled by the development of a stable isotope-labeled DNA adductomic approach involving SRM data acquisition for relative quantitation of DNA adducts induced by PR104A in cells. The analytical approach based on nanoLC−MS-SRM targeting and use of a SILAM reference mixture was useful to detect changes in the abundance of PR104A-derived DNA adducts at pharmacologically relevant levels. The results of the quantitation of PR104A-derived DNA adducts in cell lines suggest that these adducts contribute to PR104A potency, underlying the possibility of using them as biomarkers of efficacy to improve its chemotherapeutic selectivity and to stratify patients on the basis of their susceptibility to the drug. Moreover, the general DNA adductomic-SILAM approach could be adapted for relative quantitation of DNA adducts induced by any DNA alkylating agent using a stable isotope-labeled analog of the agent, but without preparation of individual labeled adducts, as a tool to support drug discovery and improve the efficacy of existing anticancer drugs.

ASSOCIATED CONTENT

Supporting Information

The Supporting Information is available free of charge on the ACS Publications website at DOI: 10.1021/acs.chemrestox.6b00412.

Full experimental details regarding cytotoxicity analysis, reaction of ctDNA with PR104A or d_4-PR104A, validation of SILAM for relative quantitation, and dGuo quantitation by HPLC; base peak accurate mass extracted ion chromatogram of DNA adducts detected in SILAM; validation of SILAM for relative quantitation by HRAM and SRM analyses in ctDNA and in DNA extracted from HT-29 cells treated with PR104A (PDF)

AUTHOR INFORMATION

Corresponding Author

*E-mail: sturlas@ethz.ch. Phone: +41 44 632 91 75. Fax: +41 44 632 11 23.

ORCID

Alessia Stornetta: 0000-0002-8287-9551

DOI: 10.1021/acs.chemrestox.6b00412
Chem. Res. Toxicol. 2017, 30, 830−839

Shana J. Sturla: 0000-0001-6808-5950

Funding

This work was supported by the Swiss National Science Foundation (31003A_156280 and CRSII3_136247), the European Research Council (260341), and the Cancer Center Support Grant No. CA-077598 and S10 RR-024618 Shared Instrumentation Grant.

Notes

The authors declare no competing financial interest.

■ ACKNOWLEDGMENTS

We gratefully acknowledge Sabine Diedrich (ETH Zurich) for technical support in cell culture, Dr. Pramod Upadhyaya (University of Minnesota) for providing a sample of d_4-O^6-POB-dG used as a reference standard, Dr. Marianna Stamou (ETH Zurich) for valuable comments regarding the manuscript, and Susanne Geisen (ETH Zurich) for technical and graphical assistance.

■ ABBREVIATIONS

A, adenine; AGC, automatic gain control; AKR1C3, aldo-keto reductase 1C3; Amu, atomic mass unit; C, cytosine; ctDNA, purified DNA from calf thymus; d_4-O^6-POB-dG, [pyridine-d_4] O^6-[4-(3-pyridyl)-4-oxobutyl-1-yl]-2′-deoxyguanosine; dGuo, deoxyguanosine; dR, 2′-deoxyribose; EC_{50}, half maximal effective concentration; G, guanine; HAP, hypoxia activated prodrug; HCEC, human colonic epithelial cells; HPLC, high performance liquid chromatography; HRAM, high-resolution/accurate-mass; Nrf2, nuclear factor erythroid 2-related factor 2; SF, sulforaphane; SILAM, stable isotope-labeled adduct mixture; SPE, solid phase extraction; SRM, selected reaction monitoring; T, thymine; U, units

■ REFERENCES

(1) Lawley, P. D., and Phillips, D. H. (1996) DNA adducts from chemotherapeutic agents. *Mutat. Res., Fundam. Mol. Mech. Mutagen. 355*, 13−40.

(2) Rajski, S. R., and Williams, R. M. (1998) DNA Cross-Linking Agents as Antitumor Drugs. *Chem. Rev. 98*, 2723−2796.

(3) Povirk, L. F., and Shuker, D. E. (1994) DNA damage and mutagenesis induced by nitrogen mustards. *Mutat. Res., Rev. Genet. Toxicol. 318*, 205−226.

(4) Wilson, W. R., and Hay, M. P. (2011) Targeting hypoxia in cancer therapy. *Nat. Rev. Cancer 11*, 393−410.

(5) Benito, J., Zeng, Z., Konopleva, M., and Wilson, W. R. (2013) Targeting hypoxia in the leukemia microenvironment. *Int. J. Hematol. Oncol. 2*, 279−288.

(6) Vaupel, P., Hockel, M., and Mayer, A. (2007) Detection and characterization of tumor hypoxia using pO2 histography. *Antioxid. Redox Signaling 9*, 1221−1235.

(7) Cheung-Ong, K., Giaever, G., and Nislow, C. (2013) DNA-damaging agents in cancer chemotherapy: serendipity and chemical biology. *Chem. Biol. 20*, 648−659.

(8) Peng, X., and Gandhi, V. (2012) ROS-activated anticancer prodrugs: a new strategy for tumor-specific damage. *Ther. Delivery 3*, 823−833.

(9) Patterson, A. V., Ferry, D. M., Edmunds, S. J., Gu, Y., Singleton, R. S., Patel, K., Pullen, S. M., Hicks, K. O., Syddall, S. P., Atwell, G. J., Yang, S., Denny, W. A., and Wilson, W. R. (2007) Mechanism of Action and Preclinical Antitumor Activity of the Novel Hypoxia-Activated DNA Cross-Linking Agent PR-104. *Clin. Cancer Res. 13*, 3922−3932.

(10) Guise, C. P., Wang, A. T., Theil, A., Bridewell, D. J., Wilson, W. R., and Patterson, A. V. (2007) Identification of human reductases that activate the dinitrobenzamide mustard prodrug PR-104A: a role for NADPH:cytochrome P450 oxidoreductase under hypoxia. *Biochem. Pharmacol. 74*, 810−820.

(11) Guise, C. P., Abbattista, M. R., Tipparaju, S. R., Lambie, N. K., Su, J., Li, D., Wilson, W. R., Dachs, G. U., and Patterson, A. V. (2012) Diflavin oxidoreductases activate the bioreductive prodrug PR-104A under hypoxia. *Mol. Pharmacol. 81*, 31−40.

(12) Singleton, R. S., Guise, C. P., Ferry, D. M., Pullen, S. M., Dorie, M. J., Brown, J. M., Patterson, A. V., and Wilson, W. R. (2009) DNA Cross-Links in Human Tumor Cells Exposed to the Prodrug PR-104A: Relationships to Hypoxia, Bioreductive Metabolism, and Cytotoxicity. *Cancer Res. 69*, 3884−3891.

(13) Stornetta, A., Villalta, P. W., Hecht, S. S., Sturla, S. J., and Balbo, S. (2015) Screening for DNA Alkylation Mono and Cross-Linked Adducts with a Comprehensive LC−MS(3) Adductomic Approach. *Anal. Chem. 87*, 11706−11713.

(14) Guise, C. P., Abbattista, M. R., Singleton, R. S., Holford, S. D., Connolly, J., Dachs, G. U., Fox, S. B., Pollock, R., Harvey, J., Guilford, P., Donate, F., Wilson, W. R., and Patterson, A. V. (2010) The bioreductive prodrug PR-104A is activated under aerobic conditions by human aldo-keto reductase 1C3. *Cancer Res. 70*, 1573−1584.

(15) Jamieson, S. M. F., Gu, Y., Manesh, D. M., El-Hoss, J., Jing, D., MacKenzie, K. L., Guise, C. P., Foehrenbacher, A., Pullen, S. M., Benito, J., Smaill, J. B., Patterson, A. V., Mulaw, M. A., Konopleva, M., Bohlander, S. K., Lock, R. B., and Wilson, W. R. (2014) A novel fluorometric assay for aldo-keto reductase 1C3 predicts metabolic activation of the nitrogen mustard prodrug PR-104A in human leukaemia cells. *Biochem. Pharmacol. 88*, 36−45.

(16) Moradi Manesh, D. M., El-Hoss, J., Evans, K., Richmond, J., Toscan, C. E., Bracken, L. S., Hedrick, A., Sutton, R., Marshall, G. M., Wilson, W. R., Kurmasheva, R. T., Billups, C., Houghton, P. J., Smith, M. A., Carol, H., and Lock, R. B. (2015) AKR1C3 is a biomarker of sensitivity to PR-104 in preclinical models of T-cell acute lymphoblastic leukemia. *Blood 126*, 1193−1202.

(17) Juge, N., Mithen, R. F., and Traka, M. (2007) Molecular basis for chemoprevention by sulforaphane: a comprehensive review. *Cell. Mol. Life Sci. 64*, 1105−1127.

(18) Erzinger, M. M., Bovet, C., Hecht, K. M., Senger, S., Winiker, P., Sobotzki, N., Cristea, S., Beerenwinkel, N., Shay, J. W., Marra, G., et al. (2016) Sulforaphane Preconditioning Sensitizes Human Colon Cancer Cells towards the Bioreductive Anticancer Prodrug PR-104A. *PLoS One 11*, e0150219.

(19) Gu, Y., Patterson, A. V., Atwell, G. J., Chernikova, S. B., Brown, J. M., Thompson, L. H., and Wilson, W. R. (2009) Roles of DNA repair and reductase activity in the cytotoxicity of the hypoxia-activated dinitrobenzamide mustard PR-104A. *Mol. Cancer Ther. 8*, 1714−1723.

(20) Hunter, F. W., Hsu, H. L., Su, J., Pullen, S. M., Wilson, W. R., and Wang, J. (2014) Dual targeting of hypoxia and homologous recombination repair dysfunction in triple-negative breast cancer. *Mol. Cancer Ther. 13*, 2501−2514.

(21) Hunter, F. W., Wang, J., Patel, R., Hsu, H. L., Hickey, A. J., Hay, M. P., and Wilson, W. R. (2012) Homologous recombination repair-dependent cytotoxicity of the benzotriazine di-N-oxide CEN-209: comparison with other hypoxia-activated prodrugs. *Biochem. Pharmacol. 83*, 574−585.

(22) Balbo, S., Turesky, R. J., and Villalta, P. W. (2014) DNA Adductomics. *Chem. Res. Toxicol. 27*, 356−366.

(23) Atwell, G. J., and Denny, W. A. (2007) Synthesis of H-3- and H-2(4)-labelled versions of the hypoxia-activated pre-prodrug 2-((2-bromoethyl)-2,4-dinitro-6-(((2-(phosphonooxy)ethyl)amino)-carbonyl)anilino)ethyl methanesulfonate (PR-104). *J. Labelled Compd. Radiopharm. 50*, 7−12.

(24) Wang, L., Spratt, T. E., Liu, X. K., Hecht, S. S., Pegg, A. E., and Peterson, L. A. (1997) Pyridyloxobutyl adduct O6-[4-oxo-4-(3-pyridyl)butyl]guanine is present in 4-(acetoxymethylnitrosamino)-1-(3-pyridyl)-1-butanone-treated DNA and is a substrate for O6-alkylguanine-DNA alkyltransferase. *Chem. Res. Toxicol. 10*, 562−567.

(25) Lao, Y., Villalta, P. W., Sturla, S. J., Wang, M., and Hecht, S. S. (2006) Quantitation of pyridyloxobutyl DNA adducts of tobacco-specific nitrosamines in rat tissue DNA by high-performance liquid

DOI: 10.1021/acs.chemrestox.6b00412
Chem. Res. Toxicol. 2017, 30, 830−839

chromatography-electrospray ionization-tandem mass spectrometry. *Chem. Res. Toxicol. 19*, 674−682.
(26) Poirier, M. C. (1997) DNA adducts as exposure biomarkers and indicators of cancer risk. *Environ. Health Persp 105*, 907−912.
(27) Stornetta, A., Zimmermann, M., Cimino, G. D., Henderson, P. T., and Sturla, S. J. (2017) DNA Adducts from Anticancer Drugs as Candidate Predictive Markers for Precision Medicine. *Chem. Res. Toxicol. 30*, 388−409.
(28) Tretyakova, N., Goggin, M., Sangaraju, D., and Janis, G. (2012) Quantitation of DNA adducts by stable isotope dilution mass spectrometry. *Chem. Res. Toxicol. 25*, 2007−2035.
(29) Tretyakova, N., Villalta, P. W., and Kotapati, S. (2013) Mass spectrometry of structurally modified DNA. *Chem. Rev. 113*, 2395−2436.
(30) Veeranki, O. L., Bhattacharya, A., Marshall, J. R., and Zhang, Y. (2013) Organ-specific exposure and response to sulforaphane, a key chemopreventive ingredient in broccoli: implications for cancer prevention. *Br. J. Nutr. 109*, 25−32.
(31) Juge, N., Mithen, R. F., and Traka, M. (2007) Molecular basis for chemoprevention by sulforaphane: a comprehensive review. *Cell. Mol. Life Sci. 64*, 1105−1127.
(32) James, D., Devaraj, S., Bellur, P., Lakkanna, S., Vicini, J., and Boddupalli, S. (2012) Novel concepts of broccoli sulforaphanes and disease: induction of phase II antioxidant and detoxification enzymes by enhanced-glucoraphanin broccoli. *Nutr. Rev. 70*, 654−665.
(33) Jaramillo, M. C., and Zhang, D. D. (2013) The emerging role of the Nrf2-Keap1 signaling pathway in cancer. *Genes Dev. 27*, 2179−2191.
(34) Noll, D. M., Mason, T. M., and Miller, P. S. (2006) Formation and repair of interstrand cross-links in DNA. *Chem. Rev. 106*, 277−301.

DOI: 10.1021/acs.chemrestox.6b00412
Chem. Res. Toxicol. 2017, 30, 830−839